ARTICLES

Formation and Characteristics of Cu Colloids from CuO Powder by Laser Irradiation in 2-Propanol

Ming-Shin Yeh, Yuh-Sheng Yang, Yi-Pei Lee, Hsiu-Fang Lee, Ya-Huey Yeh, and Chen-Sheng Yeh*

Department of Chemistry, National Cheng Kung University, Tainan, Taiwan 701, R.O.C

Received: October 26, 1998; In Final Form: June 21, 1999

The laser ablation technique has been employed to prepare Cu colloids from CuO powder in 2-propanol using wavelengths of 1064 and 532 nm. The copper colloids resulting from 1064 nm irradiation were conspicuously stable under aerobic conditions without any protective agent present. In addition to Cu particles, the formation of oxidized product, acetone, from 2-propanol was detected by gas chromatography. The discrepancy in the Cu colloidal formation between 1064 and 532 nm was analyzed on the basis of the absorptive ability of CuO powder, the results of the power dependence, and the measurements of the dose effect. The process of photoinduced coalescence that formed larger spherical particles was found to be wavelength-dependent. The stability of the Cu colloids could be the result of their near-perfect spherical shape and the effect of their larger size.

Introduction

The investigation and development of new materials has been an incessant target of scientific and industrial consideration. Nanoscale species particularly attract remarkable attention because of their unique characteristics resulting from quantum size effects.[1−4] In fact, they have shown very promising applications, such as lubricants, catalysts, and magnetic recording media.[5−7]

Among the variety of metal nanometer-sized particles, the coinage metal group, Cu, Ag, and Au, is probably studied most extensively. In general, stabilizing reagents are introduced in preparation for acquiring colloidal dispersions. In comparison with Ag and Au, copper particles are highly unstable for oxidation. According to previous studies,[8−12] Cu colloids turned yellow or green and precipitated immediately after exposure to air. Therefore, an inert gas environment is required to stabilize copper solution as well.

A number of production techniques have been reported for metallic colloids with metal salts as starting materials, such as chemical,[9−13] photochemical,[14−16] electrochemical,[17,18] radiolytic,[19,20] and sonochemical reduction.[21−23] It is known that the laser ablation technique was developed successfully as a gas-phase method for metallic and nonmetallic particle synthesis.[24,25] Henglein[26] and Cotton[27] have applied a pulsed laser to ablate pure metal targets in various solvents to form colloidal solutions. Although a copper colloidal solution with olive-green color, indicating oxidization, was obtained by irradiating copper plate in an aerobic environment,[27a] recently, we have demonstrated a new way to generate Cu colloids with salient stability from CuO powder in 2-propanol by laser ablation through 1064 nm under aerobic and protective-agent-free conditions.[28] In this paper, detailed studies of the properties of the copper solutions by this method are presented, including the results from the irradiation wavelength of 532 nm. A comparative analysis of 1064 and 532 nm particles generation was also performed.

Experimental Section

CuO powder (99.999%) with a size range of 80−100 mesh was purchased from Strem Chemicals. HPLC grade 2-propanol was used without further purification. Pyrex vials to be used as containers for forming colloidal solutions were rinsed with nitric acid followed by sonication in distilled water prior to preparation.

The colloidal Cu particles were generated by using a Nd:YAG laser (Quantel Brilliant) operated at 10 Hz. The fundamental 1064 nm and frequency-doubled 532 nm (second harmonic generation) wavelengths were selected as light sources to irradiate CuO powder. In preparation, an unfocused laser beam was conducted through the opening into the bottle containing 0.02 g of CuO powder and 5 mL of 2-propanol.

The UV−vis extinction spectra of the colloids were recorded with a UV−vis spectrophotometer (Hewlett-Packard 8452A). The average diameters and the size distributions of the copper particles were obtained from the enlarged photographs of a transmission electron micrograph (Hitachi FE-2000 and ZEISS 10C). Electron micrographs were carried out using a drop of the sample onto a copper mesh coated with an amorphous carbon film, which was then dried in a vacuum desiccator. X-ray powder diffraction data were collected on a Rigaku (D/Max IIB) diffractometer using Cu Kα radiation ($\lambda = 1.54056$ Å) at 30 kV and 20 mA. Because an intense pulsed laser was employed to form colloidal solutions, gas chromatography

* To whom correspondence should be addressed. E-mail address: csyeh@mail.ncku.edu.tw.

10.1021/jp984163+ CCC: $18.00
Published on Web 08/03/1999

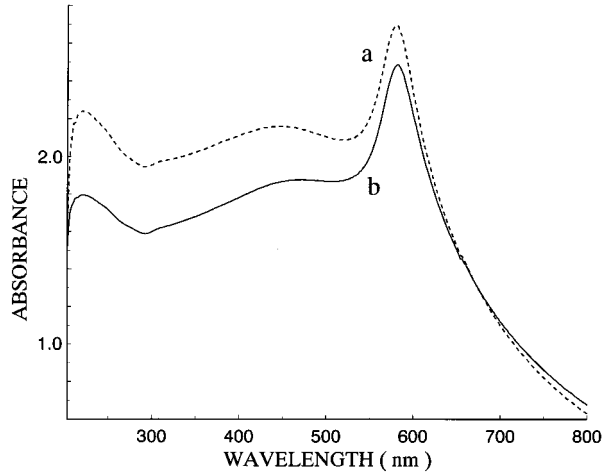

Figure 1. UV−vis absorption spectra of copper colloids prepared in 2-propanol by 1064 nm laser light with 100 mJ/pulse: (a) 5 min of irradiation; (b) additional 5 min of irradiation time for (a) colloidal solutions.

(CARLO ERBA HRGC-5300) was utilized to analyze the side reaction product.

Results

Formation of Cu Colloids at 1064 nm. Figure 1 shows the UV−vis spectra of copper colloids in 2-propanol. A characteristic peak of absorbance at 580 nm is due to the surface plasmon band of Cu colloids.[8−12,29] A laser fluence of 100 mJ/pulse (509 mJ/cm^2) was used for only 5 min to acquire deep-wine-red solutions. Prior to the measurement of optical absorption spectra,the ablated solutions were centrifuged to remove the rest of CuO powder. We also irradiated the colloidal solutions of Figure 1a, which no longer contained CuO powder, with the same laser power for an additional 5 min. The solutions became reddish pink. A wine-red colloidal solution was obtained showing plasmon excitation at 580 nm with less absorbance, as illustrated in Figure 1b.

Parts a and b of Figure 2 display the corresponding TEM images for the colloids shown in curves a and b of Figure 1, respectively. From the transmission electron micrographs, most of the particles with sizes larger than 10 nm became greater than 15 nm and the average diameter increased from 28.9 to 55.9 nm upon going to Figure 2b from Figure 2a. These results suggest that the photoinduced coalescence produced larger particles in the second stage of irradiation (Figure 1b). Thus, the descending absorption of Figure 1b was caused by fewer particles per unit volume in solution. Conversely, the magnitude of the plasmon peak grew progressively upon an increase of the particle size at fixed concentration as shown in previous theoretical studies.[30,31]

X-ray diffraction (XRD) data were collected to identify the colloids. The XRD pattern (Figure 3a) was acquired from the sample after the two-stage irradiation. The diffraction peaks at 43.2° (43.3°), 50.3° (50.3°), and 74° (73.8°) correspond to the formation of metallic copper, where the numbers in parentheses are 2θ of standard Cu. Electron diffractions (not shown) also revealed that Cu particles had formed. The same results were also obtained through single-stage illumination (Figure 1a).

Because high peak power of a pulsed laser was employed in this experiment, a side reaction product might have been generated during ablation. Although ^{1}H NMR measurements showed no species other than 2-propanol in solutions, the generation of a small amount of oxidized product, acetone, was

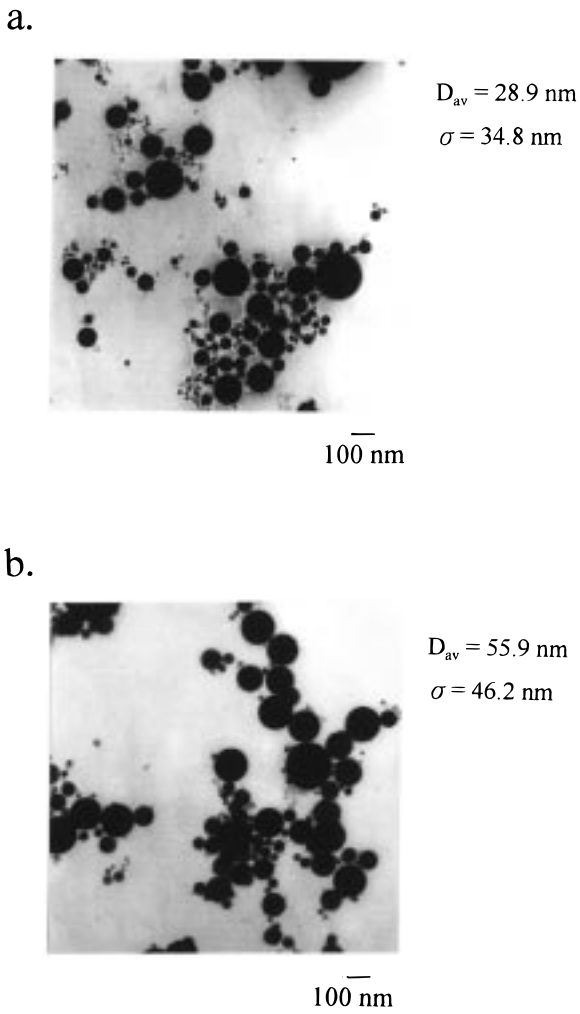

Figure 2. TEM images, with parts a and b corresponding to parts a and b of Figure 1, respectively.

confirmed by gas chromatography. Quantitatively, concentrations of acetone were 52.3 and 58.7 ppm for single-stage and second-stage irradiation, respectively. Both stages produced copper colloids and acetone, but the production yield of the acetone was reduced in the second-stage preparation. The generation of acetone in the second stage can be interpreted as electron transfer from 2-propanol to Cu particles with the copper particles acting as catalyst, where 1-hydroxymethylethyl radicals are assumed as intermediates to donate electrons. This process has been discussed in experiments using Ag and Au particles.[32,33]

As mentioned earlier, all of the experiments were performed without any precautions taken, such as under protective agents and oxygen-free conditions. Surprisingly, copper colloids made either by first-stage or second-stage irradiation exhibited much better stability than those of previous reports.[8−12] During aging, samples were stored in Pyrex bottles with caps sealed under aerobic conditions. Figure 4 shows the results of studies on the stability of solutions produced by second-stage illumination. After aging for 5 days (Figure 4b), the surface plasmon peak was red-shifted only 6−8 nm without distinct broadening and with less absorbance. The colloidal solutions still exhibited a wine-red color, while some precipitates were observed. For the aging solutions, we applied a laser output of 150 mJ/pulse for 10 min (first reverse). It was observed that the precipitates disappeared and the absorption intensity of the plasmon excitation increased and was blue-shifted to 580 nm, as illustrated in Figure 4c. Figure 4d displays the optical absorption of aging 5

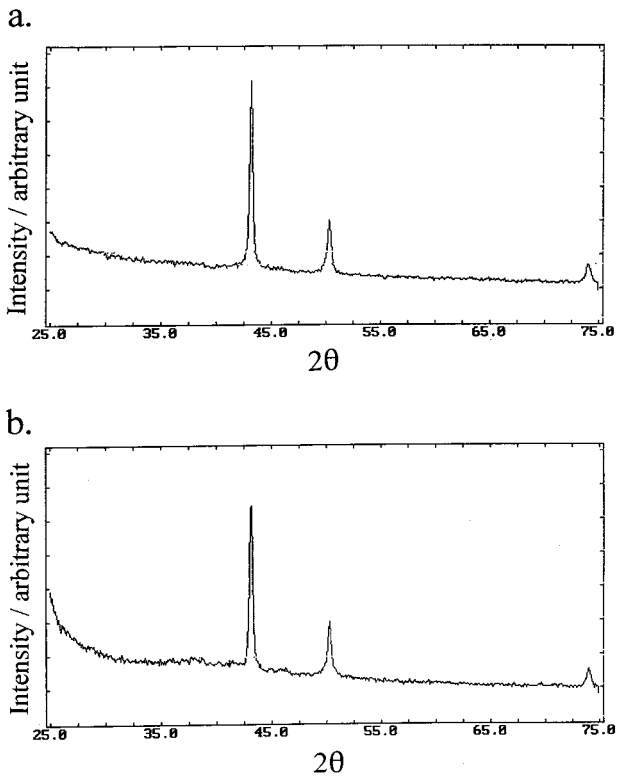

Figure 3. X-ray diffractograms of copper colloids: (a) collected from the solutions of Figure 1b; (b) acquired from the solutions of Figure 4f.

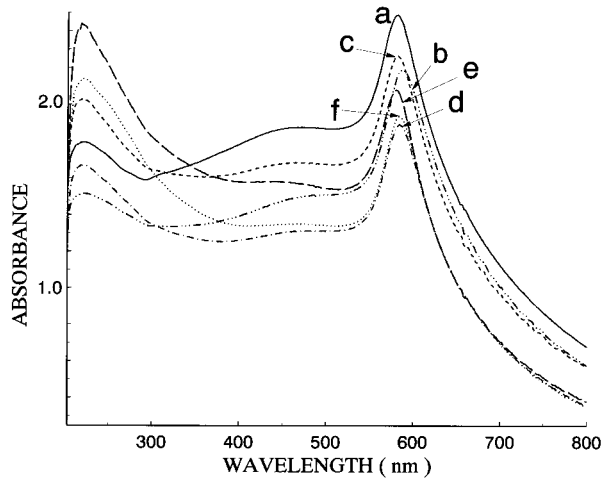

Figure 4. UV−vis spectra of copper colloids prepared in 2-propanol by 1064 nm wavelength: (a) preparation through two-stage irradiation (−); (b) absorption after aging 5 days for (a) solutions (− ···), (c) absorbance by illuminating (b) solutions for 10 min with laser intensity of 150 mJ/pulse (- - -); (d) absorption after aging 5 days for (c) solutions (− · −); (e) absorbance by illuminating (d) solutions for 10 min with laser intensity of 150 mJ/pulse (− − −); (f) absorption after aging 3 weeks for (e) solutions (···).

days relative to the spectrum of Figure 4c. Once again, the plasmon peak showed no apparent broadening and shifted 2−4 nm to the red. This seems to suggest that the speed of the oxidization and aggregation lessened after employing laser light. By use of the same laser fluence and exposure time as in Figure 4c to illuminate the solutions of Figure 4d, similar results were obtained, as shown in Figure 4e (second reverse). To verify the phenomenon of the deferred oxidization, the colloidal solutions of Figure 4e were aged for 3 weeks. In Figure 4f, it is evident that the 580 nm characteristic plasmon band shifted to a higher wavelength for merely 4 nm with no sign of changing

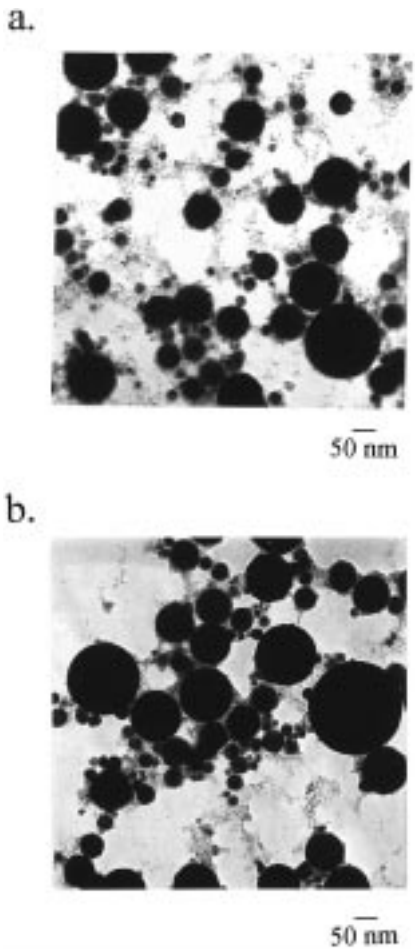

Figure 5. Transmission electron micrographs, with parts a and b obtained by applying 1064 nm wavelength at 150 mJ/pulse to the aging solutions of the one-stage and two-stage preparations, respectively.

bandwidth. All of the above observations appeared during single-stage irradiation as well.

In Figure 4, we have shown that the colloidal solutions revealed a trend of increasing stability by illuminating aged solutions. Parts a and b of Figure 5 represent the TEM views of the first reverse for first-stage and second-stage irradiation, respectively. It is clear that many smaller particles with sizes around 5−7 nm were generated compared to the colloids prepared as in Figure 2. This is indicative of disintegrating particles after introducing laser light to the aged colloids. It can be seen that the absorbance increased progressively, as depicted in curves c and e of Figure 4. It is known that the absorption in the UV excitation is due to the interband transition and is insensitive to the effect of the particle size but is sensitive to the proportion of the volume of particles. Therefore, the increasing particle quantity results in the growth of the absorbance in the UV region. It can be seen from the electron microscopy photographs that the periphery of larger particles is surrounded by small particles. If smaller particles reveal higher activity, these small species are very possibly copper oxides and/or an oxide layer formed on particle surfaces. Figure 3b displays the XRD pattern obtained from the colloidal solutions of Figure 4f. In addition to the strong Cu diffraction peaks, there is a bulge between 35° and 39°. It is noted that $Cu_2O(111)$, 36.5°, and CuO(111), 38.7°, are located in this region. Selected area electron diffractions for these fine particles showed a diffuse ring, indicating an amorphous structure; in some specimens a $Cu_2O(111)$ reflection appeared. One can conceive that the oxide

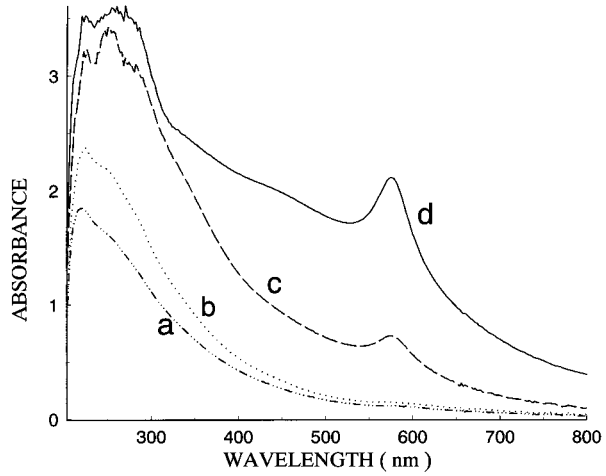

Figure 6. Optical absorption measured at various laser powers and exposure times for 532 nm wavelength: (a) laser power of 50 mJ/pulse for 10 min; (b) laser power of 50 mJ/pulse for 30 min; (c) laser power of 115 mJ/pulse for 30 min; (d) additional 30 min under 300 mJ/pulse energy for (c) colloids.

shells, formed by these small particulates, surrounded the large particles to prevent aggregation and to stabilize Cu colloids.

Formation of Cu Colloids by 532 nm. To compare with IR light, the 532 nm light was chosen to study the wavelength dependence of the Cu colloidal formation. Figure 6 represents the optical absorption measured through the variation in laser power and irradiation time. Figure 6d was measured by illuminating the colloidal solutions of Figure 6c, where no more CuO powder was present, for an additional 30 min under 300 mJ/pulse of laser intensity. The characteristic peak of 576 nm grew progressively by increasing laser fluence and exposure time. Parts a−c of Figure 7 display the corresponding TEM images shown in curves b−d of Figure 6, respectively. It is obvious that higher laser power and longer exposure time caused the growth of the particle sizes. In comparison with results with 1064 nm, Figure 7c reveals a smaller average diameter of 24.7 nm with a standard deviation [σ] of 11.4 nm and a tendency to coagulate. Most of particles with sizes less than 10 nm were generated under the operating conditions of Figure 7b, and sizes even smaller than 1 nm were obtained in Figure 7a. A wine-red solution will be acquired under the operating conditions used in Figures 6d and 7c. However, the colors light-yellow, yellow, and brown appeared in sequence from Figure 6a to Figure 6c, indicating oxidation. The corresponding electron diffraction exhibited the reflection of $Cu_2O(111)$.

The Cu colloids with the wine-red color made through 532 nm were not as stable as those produced through 1064 nm, as illustrated in Figure 8. After aging 5 days, the surface plasmon shifted to 600 nm and showed significant broadening. In fact, the color turned to blue gradually after 2 days. We used 532 nm wavelength with 300 mJ/pulse to irradiate aging solutions for 30 min. Although a wine-red appearance emerged, the surface plasmon position (580 nm) was not quite brought back to 576 nm and was accompanied by a long tailing toward longer wavelengths. The TEM photographs showed that they exhibited

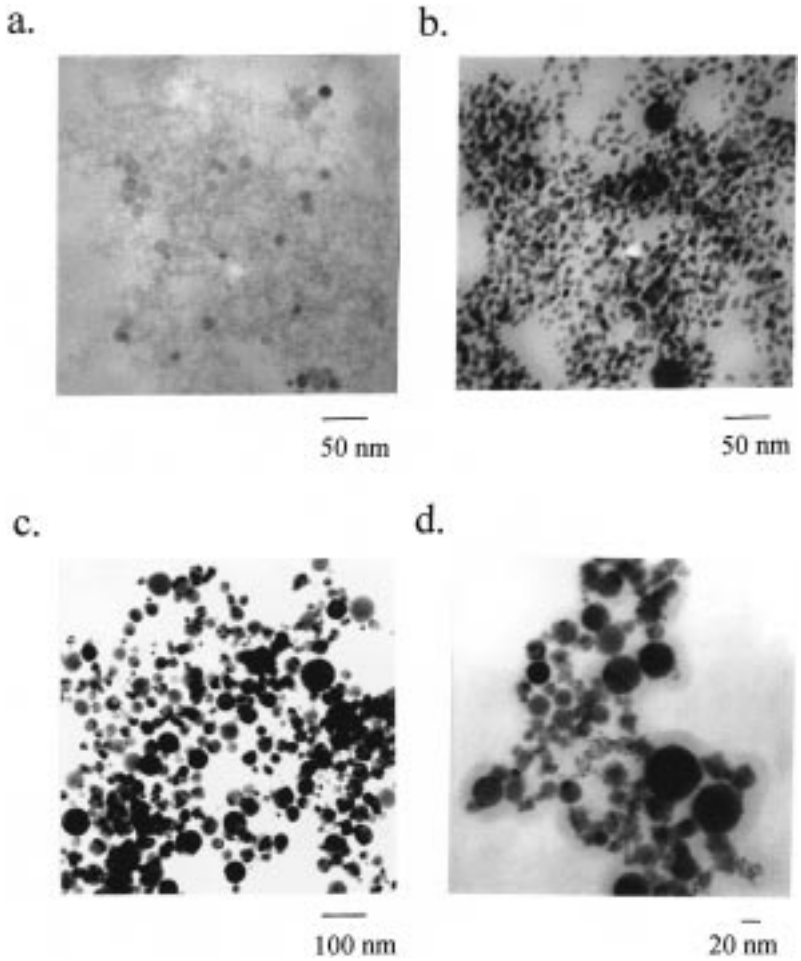

Figure 7. Transmission electron images corresponding to (a) the colloids of Figure 6b, (b) the colloids of Figure 6c, (c) the colloids of Figure 6d, (d) the colloids of Figure 8c.

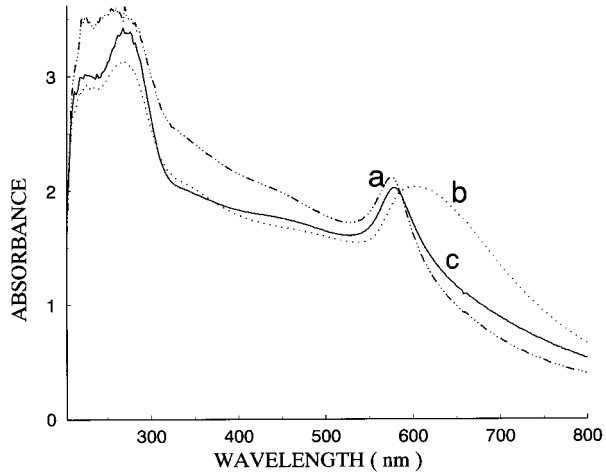

Figure 8. Stability of Cu colloids made in 532 nm: (a) wine-red solutions of Figure 6d; (b) after aging of (a) colloidal solutions for 5 days; (c) after irradiation of (b) colloidal solution for 30 min with laser output of 300 mJ/pulse.

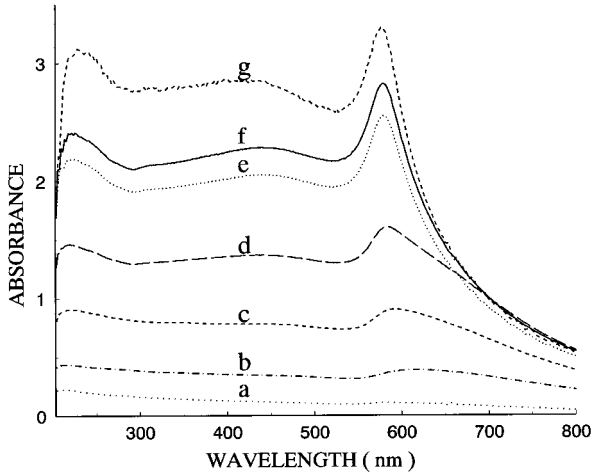

Figure 9. Absorption spectra at various laser fluences of 1064 nm under exposure time of 5 min: (a) 30 mJ/pulse, (b) 40 mJ/pulse, (c) 50 mJ/pulse, (d) 70 mJ/pulse, (e) 80 mJ/pulse, (f) 90 mJ/pulse, (g) 100 mJ/pulse

clumps with diffuse contours constituting a lot of small and/or amorphous particles, as shown in Figure 7d. The reversed colloids precipitated completely after 4−5 days.

Although the absorbance in the UV region (200−300 nm) displayed saturation in Figure 8a, a maximum appearing around 270 nm was observed after the reduction of the absorption intensity. It is known that acetone has an absorption band at 272 nm. Gas chromatography detected acetone at 4.1×10^3 ppm. With the same light intensity and irradiation time, we found that more acetone was generated by 532 nm than by 1064 nm. This is related to more particles being produced at 532 nm.

Discussion

Investigations were performed to understand the desorption mechanisms that result from the interaction of the laser light with metal or nonmetal materials.[34−37] Both thermal and/or electronic excitation effects were considered for the photodesorption process. These results were all acquired in an ultrahigh vacuum environment. Although a laser was also utilized to irradiate CuO powder in these studies, the solvent was employed as a medium to form nanoproducts, Cu colloids. To our knowledge, there has been no report that discusses the colloidal formation mechanism by laser ablation in solvent. Therefore, we have attempted to understand the factors that affect particle formation, such as power dependence and dose effect, and by comparing the results from 1064 and 532 nm.

As mentioned earlier, the 1064 nm wavelength has been demonstrated to be the best candidate to generate stable Cu colloids. However, green light (532 nm) was found to generate particles more efficiently. Power dependence was studied for both wavelengths. The threshold of the colloidal formation is 20 mJ/pulse of laser fluence at 1064 nm, while 532 nm can be used as low as 10 mJ/pulse for particle production. The laser diameter (0.5 cm) was constant throughout the experiments. With the same laser power, the wavelength of 1064 nm has a large photon flux (photons/cm^2). Since both wavelengths are able to yield colloids, one would expect a larger photon flux to deposit more energy into CuO powder and to complete this process more easily. If we inspect absorptive ability of CuO for 1064 and 532 nm, the discrepancy between photon flux and the onset of producing particles may be understood. It was found that the absorption coefficient ($\sim 2.5 \times 10^5$ cm^{-1}) at 532 nm is 5 times that of CuO at 1064 nm.[38] Therefore, this is possibly the reason that 532 nm can generate particles at lower fluence.

Figure 9 displays the optical absorption spectra of the colloidal solutions at various fluences of 1064 nm. The illumination time was maintained at 5 min. Two distinct absorbance shapes were observed. The copper plasmon bands showing broadening and tailing toward longer wavelengths appeared below 80 mJ/pulse of laser intensity, whereas the sharp and narrow plasmon peaks were obtained once the fluence was greater than 70 mJ/pulse. The colors of the colloids were easily distinguishable. From 40 to 70 mJ/pulse, they were mixed with blue and red, the red component turning deeper as the power increased. This indicates that colloids containing copper and copper oxides have been produced. The electron diffraction patterns confirmed the coexistence of both Cu and Cu_2O rings. A transparent solution was observed at 30 mJ/pulse because there were much fewer particles in solution. Above 70 mJ/pulse, wine-red solutions with Cu colloids were acquired. These results show that larger photon flux is necessary to make pure copper without oxide particles and that a multiphoton process is required for formation of Cu colloids by 1064 nm.

On the basis of the above observations, 532 nm should be a good choice to form Cu colloids because of the higher photon energy and better absorptive ability of CuO powder; unfortunately, it is not. Single laser dosage experiments were designed for 1064, 532, and 355 nm. The laser intensity was chosen at 100 mJ/pulse, which was enough to have pure Cu particles made at 1064 nm. Figure 10 shows that a shorter wavelength generated more numerous and smaller particles, exhibiting oxidization. Apparently, small particles display higher reactivity to being oxidized. It might be that the energies of 532 and 355 nm were just too high to yield stable Cu colloids. For 1064 nm, the particles with almost spherical shapes were already formed under a 5 ns pulse width.

To produce a wine-red solution containing Cu colloids, a high power, i.e., 300 mJ/pulse, laser beam was employed in a second-stage irradiation. The results are shown in Figures 6d and 7c and can be attributed to the low absorption of the oxidized colloids. Either the surface oxide layer on the Cu particles or oxidized Cu (Cu_2O) has an absorption coefficient less than 20 cm^{-1}.[39] After being irradiated, the oxidized species began reduction as the Cu and the brown color gradually changed to red starting from the upper layer of solution. Because of the longer illumination time used for 532 nm than for 1064 nm,

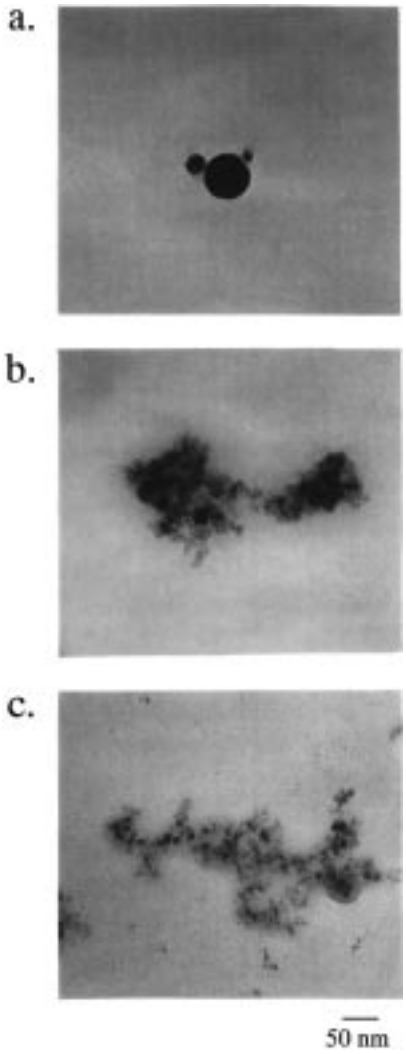

Figure 10. TEM images of one laser pulse of 1064 nm (a), 532 nm (b), and 355 nm (c) with laser output of 100 mJ/pulse.

the increasing concentration of particles in solution caused aggregation to become serious, as seen in parts a−c of Figure 7.

By use of 1064 nm, the phenomenon of the photoinduced coalescence was observed in the second-stage preparing procedure, as depicted in Figure 1b. Kimura reported that photoinduced coagulation results from enhanced van der Waals for the interparticle interaction in an electromagnetic field.[40] The frequency of plasmon oscillation and smaller particle size will promote this effect dramatically. However, spherical shapes rather than the irregular aggregation of the particles, as reported in previous research, were produced in our studies. An enhanced van der Waals force seems to be unsuited to explain what we observed. The experiments were conducted by using 532 or 355 nm at the second-stage illumination. The resulting solutions appeared yellow and the plasmon band became ambiguous. TEM images showed that particles had disintegrated and turned into amorphous structures. Hence, photoinduced coalescence is wavelength-dependent, but the reason(s) remains unclear.

Although we have presented some explanations pertaining to Cu colloidal formation for different wavelengths, no information is available to provide the mechanism of how CuO powder interacts with a pulsed laser to form Cu in the nanophase. An interesting clue was the appearance of Cu_2O and Cu in the CuO powder that was removed from solution. Figure 11 exhibits XRD measurements of pure CuO powder without illumination by laser and of the powders with 1064 and 532 nm irradiation. The peaks without labeling are CuO reflections. On the basis of these results, one possibility for production of Cu nanoparticles is

$$CuO_{(b)} \rightarrow Cu_2O_{(b)} \rightarrow Cu_{(b)} \rightarrow Cu_{(n)} \qquad (1)$$

where b stands for bulk phase and n represents nanophase.

The production of the acetone can then be involved in the release of oxygen with the 2-propanol reaction. However, the next question is how the oxygen was liberated from CuO. Would the e^-−hole pairs be generated and the relaxed holes be diffused to the surface with resulting neutralization of oxygen ions followed by the loss of the oxygen, which resembles the sputtering process in oxides?[41] Another important point is why the 1064 nm is able to yield particles with near-perfect spherical shapes and how this process can proceed completely in a period of 5 ns. It should be noted that there is no direct evidence to support the above-mentioned formation sequence (1), and the true mechanism may be more complicated.

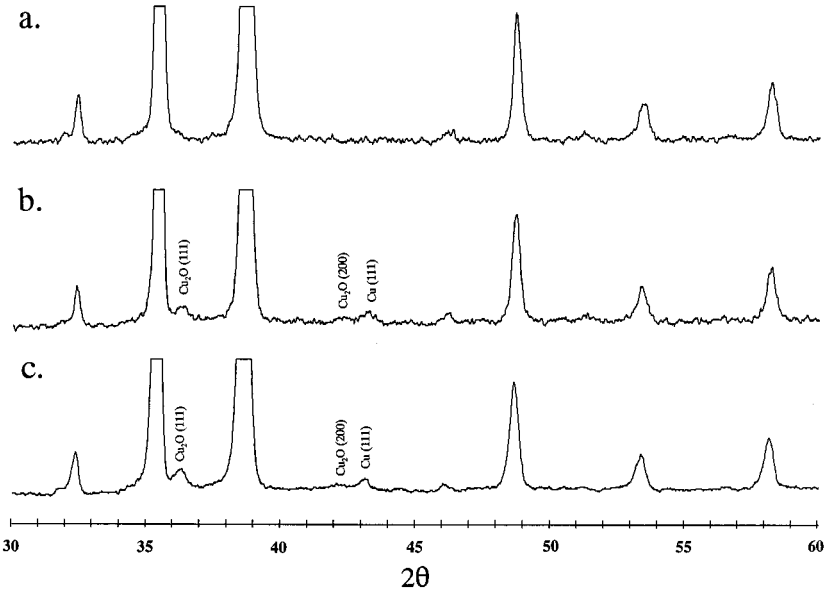

Figure 11. XRD data of CuO samples: (a) powders without being irradiated; (b) powders irradiated by 1064 nm at 100 mJ/pulse for 5 min; (c) powders irradiated by 532 nm at 100 mJ/pulse for 5 min.

We have shown that copper colloids made by 1064 nm were conspicuously stable without protective agents in an aerobic environment. From parts a and b of Figure 2, the average particle diameters of 28.9 and 55.9 nm for both first-stage and second-stage preparations were significantly larger than those of previous studies, although a few cases generated sizes of less than 10 nm.[8−12] The unusual stability of the Cu colloids is possibly due to their larger less active sizes. In addition to the size effect, the near-perfect spherical shape probably contributes significantly to stability. Because this configuration has the least surface tension and is the most thermodynamically stable, small particles with sizes 10−15 nm in parts a and b of Figure 2 were even stable against air.

Conclusion

The conspicuously stable Cu colloids with larger mean sizes were produced under aerobic and protective-agent-free conditions by illuminating CuO powder in 2-propanol through 1064 nm. The production and the properties of the Cu particles displayed wavelength dependence. Moreover, in these studies, two potential issues have been brought up: (a) the formation mechanism from bulk phase to nanophase by laser ablation with solvent as medium and (b) the property of the colloids after interacting with the high peak power of the laser. They are worthy of further investigation.

The method presented here may also provide an alternative route to explore metal nanoscale materials from the bulk phase of metal oxides. The colloids prepared in this experiment offer an opportunity to conveniently and directly probe the surface-enhanced Raman scattering (SERS) without the influence of ions or stabilizer reagents, which is currently under study.

Acknowledgment. This work is partially supported by the National Science Council of the Republic of China. We acknowledge Dr. Jacob Chun-Hsiung Kuei for lending the gas chromatograph to us, Mr. S. Y. Yao and Ms. S. Y. Hsu for carrying out TEM measurements, and Mr. Jen-Min Chen for providing XRD data collections at Tainan Regional Instrument Center, National Cheng Kung University.

References and Notes

(1) Nojik, A. J.; Williams, F.; Menadovic, M. T.; Rajh, T.; Micic, O. E. *J. Phys. Chem.* **1985**, *89*, 397.
(2) Halperin, W. P. *Rev. Mod. Phys.* **1986**, *58*, 533.
(3) Henglein, A. *Chem. Rev.* **1989**, *89*, 1861.
(4) Bawendi, M. G.; Steigerwald, M. L.; Brus, L. E. *Annu. Rev. Phys. Chem.* **1990**, *41*, 477.
(5) Rapoport, L.; Billk, Y.; Feldman, Y.; Homyonfer, M.; Cohen, S. R.; Tenne, R. *Nature* **1997**, *387*, 791.
(6) Henglein, A. *J. Phys. Chem.* **1980**, *84*, 3461.
(7) Majetich, A.; Artman, J. O.; McHenry, M. E.; Nuhfer, N. T.; Staley, S. W. *Phys. Rev. B* **1993**, *48*, 16845.
(8) Kimura, K. *Bull. Chem. Soc. Jpn.* **1984**, *57*, 1683.
(9) (a) Hirai, H.; Wakabayashi, H.; Komiyama, M. *Chem. Lett.* **1983**, 1047. (b) Hirai, H.; Wakabayashi, H.; Komiyama, M. *Bull. Chem. Soc. Jpn.* **1986**, *59*, 367.
(10) Lisiecki, I.; Pileni, M. P. *J. Am. Chem. Soc.* **1993**, *115*, 3887.
(11) Curtis, A. C.; Duff, D. G.; Edwards, P. P.; Jefferson, D. A.; Johnson, B. F. G.; Kirkland, A. I.; Wallace, A. S. *J. Phys. Chem.* **1988**, *92*, 2270.
(12) Huang, H. H.; Yan, F. Q.; Kek, Y. M.; Chew, C. H.; Xu, G. Q.; Ji, W.; Oh, P. S.; Tang, S. H. *Langmuir* **1997**, *13*, 172.
(13) Ahmadi, T. S.; Wang, Z. L.; Green, T. C.; Henglein, A.; El-Sayed, M. A. *Science* **1996**, *272*, 1924.
(14) Toshima, N.; Takahashi, T.; Hirai, H. *Chem. Lett.* **1985**, 1245.
(15) Ohtaki, M.; Toshima, N. *Chem. Lett.* **1990**, 489.
(16) Huang, H. H.; Ni, X. P.; Loy, G. L.; Chew, C. H.; Tan, K. L.; Loh, F. C.; Deng, J. F.; Xu, G. Q. *Langmuir* **1996**, *12*, 909.
(17) Reetz, M. T.; Helbig, W. *J. Am. Chem. Soc.* **1994**, *116*, 7401.
(18) Anderson, M. A.; Gorer, S.; Penner, R. M. *J. Phys. Chem. B* **1997**, *101*, 5895.
(19) Gutiérrez, M.; Henglein, A. *J. Phys. Chem.* **1993**, *97*, 11368.
(20) Zhang, H.; Mostafavi, M. *J. Phys. Chem. B* **1997**, *101*, 8443.
(21) Gutiérrez, M.; Henglein, A. *Ultrasonics* **1989**, *27*, 259.
(22) Nagata, Y.; Watananabe, Y.; Fujita, S. I.; Dohmaru, T.; Taniguchi, S. *J. Chem. Soc., Chem. Commun.* **1992**, 1620.
(23) Mizukoshi, Y.; Okitsu, K.; Maeda, Y.; Yamamoto, T. A.; Oshima, R.; Nagata, Y. *J. Phys. Chem. B* **1997**, *101*, 7033.
(24) Guo, T.; Nikolav, P.; Thess, A.; Colbert, D. T.; Smalley, R. E. *Chem. Phys. Lett.* **1995**, *243*, 49.
(25) Morales, A.; Lisber, C. M. *Science* **1998**, *279*, 208.
(26) Fojtik, A.; Henglein, A. *Ber. Bunsen-Ges. Phys. Chem.* **1993**, *97*, 252.
(27) (a) Neddersen, J.; Chumanov, G.; Cotton, T. M. *Appl. Spectrosc.* **1993**, *47*, 1959. (b) Sibbald, M. S.; Chumanov, G.; Cotton, T. M. *J. Phys. Chem.* **1996**, *100*, 4672.
(28) Yeh, Y. H.; Yeh, M. S.; Lee, Y. P.; Yeh, C. S. *Chem. Lett.* **1998**, 1183.
(29) Abe, H.; Charlé, K. P.; Tesche, B.; Schulze, W. *Chem. Phys.* **1982**, *68*, 137.
(30) Ruppin, R. *J. Appl. Phys.* **1986**, *59*, 1355.
(31) Lisiecki, I.; Billoudet, F.; Pileni, M. P. *J. Phys. Chem.* **1996**, *100*, 4160.
(32) Takeuchi, Y.; Ida, T.; Kimura, K. *J. Phys. Chem. B* **1997**, *101*, 1322.
(33) Henglein, A. *J. Phys. Chem.* **1993**, *97*, 5457.
(34) Hoheisel, W.; Schulte, U.; Vollmer, M.; Träger, F. *Appl. Phys. A* **1990**, *51*, 271.
(35) Lee, I.; Parks, J. E., II; Callcott, T. A.; Arakawa, E. T. *Phys. Rev. B* **1989**, *39*, 8012.
(36) Srinivasan, R. *Science* **1986**, *234*, 559.
(37) Chuang, T. J.; Hussla, I. *Phys. Rev. Lett.* **1984**, *52*, 2045.
(38) Tanaka, T. *Jpn. J. Appl. Phys.* **1979**, *18*, 1043.
(39) Yanase, A.; Komiyama, H. *Surf. Sci.* **1991**, *248*, 11.
(40) (a) Satoh, N.; Hasegawa, H.; Tsujii, K.; Kimura, K. *J. Phys. Chem.* **1994**, *98*, 2143. (b) Kimura, K. *Bull. Chem. Soc. Jpn.* **1996**, *69*, 321. (c) Kimura, K. *J. Phys. Chem.* **1994**, *98*, 11997.
(41) Kelly, R. *Surf. Sci.* **1979**, *90*, 280.